

# Robot-musculoskeletal dynamic biomechanical model in robot-assisted diaphyseal fracture reduction

Changsheng Li<sup>a</sup>, Tianmiao Wang<sup>a</sup>, Lei Hu<sup>a,\*</sup>, Lihai Zhang<sup>b</sup>, Yanpeng Zhao<sup>b</sup>, Hailong Du<sup>b</sup>, Lifeng Wang<sup>a</sup> and Peifu Tang<sup>b,\*</sup>

<sup>a</sup>*School of Mechanical Engineering and Automation, Beihang University, Beijing, China*

<sup>b</sup>*Department of Orthopaedics, Chinese PLA General Hospital, Beijing, China*

**Abstract.** A number of issues that exist in common fracture reduction surgeries can be mitigated by robot-assisted fracture reduction. However, the safety of patients and the performance of the robot, which are closely related to the muscle forces, are important indexes that restrict the development of robots. Though researchers have done a great deal of work on the biomechanics of the musculoskeletal system, the dynamics of the musculoskeletal system, particularly the aspects related to the function of the robot, is not well understood. For this reason, we represent the complex biological system by establishing a dynamic biomechanical model based on the Hill muscle model and the Kane method for the robot that we have developed and the musculoskeletal system. We analyzed the relationship between the motion and force of the bone fragments and the robot during a simulation of a robot-assisted fracture reduction. The influence of the muscle force on the robot system was predicted and managed. The simulation results provide a basis for a fracture reduction path plan that ensures patient safety and a useful reference for the mechanical design of the robot.

Keywords: Robot-assisted diaphyseal fracture reduction, musculoskeletal system, biomechanical model, simulation analysis

## 1. Introduction

The traditional surgical treatment for diaphyseal fracture is open reduction. This method provides accurate reduction but relies extensively on the surgeon's expertise. The exposure of the fractured location could cause delayed union or nonunion because of the destruction of the blood supply, which causes secondary injury to patients [1]. Intramedullary nailing is an effective method for reducing patient injury [2], but it exhibits some disadvantages. For example, the intraoperative X-ray guidance could irradiate patients and surgeons who frequently perform such surgeries. Additionally, the two-dimensional X-ray data lack information in the depth direction, which leads to rotational errors [3, 4].

With the development of robotics and artificial intelligence, researchers have developed the robot-

---

\*Address for correspondence: Lei Hu, School of Mechanical Engineering and Automation, Beihang University, No. 37, Xueyuan Road, Haidian District, Beijing, 100191, China. Tel.: +86 10 8233 8272; Fax: +86 10 8233 8272; E-mail: [hulei9971@sina.com](mailto:hulei9971@sina.com).

Peifu Tang, Department of Orthopaedics, Chinese PLA General Hospital, No. 28, Fuxing Road, Haidian District, Beijing, 100853, China. Tel.: +86 10 6693 9130; Fax: +86 10 6821 2342; E-mail: [kico\\_dredd@hotmail.com](mailto:kico_dredd@hotmail.com).

assisted fracture reduction systems to mitigate the above disadvantages [5-7]. During the fracture reduction, it is very important to ensure the safety of patients who are operated upon by robots. The main factors that influence safety are related to the patient, such as the resistance provided by the body, rather than to the robot. According to human anatomy, the diaphysis is surrounded by large amounts of muscle, nerve tissue and soft tissue. The resistance to reduction comes primarily from the muscle force. For example, the resistance to the femur reduction in the axial direction can be as high as 411 N [8]. If the reduction path is not planned reasonably, the resistance could be sufficiently large to injure the muscle and soft tissue, especially the nervous tissue, thereby causing irreversible nerve and tissue damage. The accuracy and stability of the robot could also be affected by the resistance, which is a challenge in the design of the robot. In addition, the fragments and the robot are connected as a whole, with relationships between their forces and motions. As a result, the dynamics of the robot-musculoskeletal system during the reduction must be studied.

The musculoskeletal system is difficult to study because of the complexity of the muscle and the risk of invasiveness due to the human's particularity. The difficulty is increased upon considering the robotic factors. Modeling and simulation provide effective solutions. Current research investigates the biomechanical modeling of the complete musculoskeletal system [9]. In 1990, Delp, et al. [10] established a relatively complete musculoskeletal model of the lower limb. In 2010, E. Ma, et al. [11] measured the muscular shape of a corpse to obtain data to modify the musculoskeletal model. Some researchers established musculoskeletal model by motion capture technique [12]. The above studies are very mature. Compared with traditional fracture reduction surgery, the robot does not allow a surgeon to perceive the state of the patient in real time and make accurate judgments in robot-assisted fracture reduction. As a result, the dynamics of both the robot and the fragments is very important. It is also proved to be a grand challenge in the field of musculoskeletal [13, 14]. The robot-assisted fracture reduction system has only been developed recently and remains relatively unstudied. Similar studies, such as that by Rolf Westphal, et al. [8] measured the force and the torque of the reduction, but the relationship between the operation force and the motion of the fragments was not detailed. Xie, et al. [15] researched the biomechanics of reduction, but the dynamics were not studied considering the robot factors.

The model of the robot-musculoskeletal system that we have established is based on the robot system that we developed for diaphyseal fracture reduction [16, 17]. This paper is organized as follows. The following section describes the robot system we developed. Subsequently, we propose the robot musculoskeletal system model and present some results based on the simulation. Finally, we outline the results, give a conclusion and a prospect of future work.

## 2. Materials and methods

### 2.1. Robot system for diaphyseal fracture reduction

The robot system shown in Figure 1 mainly includes a fixing support, a reduction mechanism and a control system. Generally speaking, the fractured diaphysis is divided into two parts: a proximal fragment and a distal fragment. These fragments need to be connected to the fixing support by Schanz screws. The fixing support is connected to the reduction mechanism by a fast connector. The reduction mechanism is a Stewart mechanism with six degrees of freedom (6-DOF), which can provide high accuracy and a large force. It is used to drive the distal fragment to conduct a fracture reduction operation under the guidance of the control system. The control system includes a personal

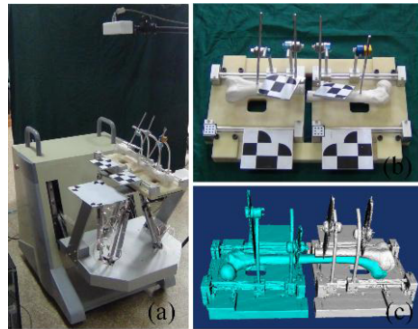


Fig. 1. Robot system for diaphyseal fracture reduction: (a) the robot system; (b) the fixing support; (c) the 3D-CT data of the fragments and the fixing support

computer (PC, Intel(R) Core(TM) i5-3340M CPU @ 2.70 GHz) with the operation system of Windows 7 that runs the software to handle the CT data and control the motion of the robot, drivers and a visual servo system based on a Micro Tracker (Claron Technology Inc., Canada). The feasibility of the robot system has been verified by experiments based on model bones and animal bones in previous studies.

The fracture reduction method is as follows. First, we obtain 3D-CT data of the fractured fragments with the fixing support and the contralateral diaphysis using CT scans. Subsequently, the fixing support must be connected to the reduction mechanism. The distal fragment is fixed on the Stewart mechanism, and the proximal fragment is fixed on the body of the robot system. Next, the 3D-CT data are divided into three parts in the PC: the proximal fragment, the distal fragment and the contralateral diaphysis. The contralateral diaphysis is taken as a reference. The pose of the distal fragment relative to the proximal fragment is obtained by registration. Finally, the CT coordinate system needs to be transformed to the robot system. The driving rod length of the Stewart mechanism can be obtained by inverse kinematics for the control of the robot system.

The shortening of the fracture fragments can be caused by the muscle contraction force. Therefore, the distal fragment needs to be stretched along its axial direction to reduce the possibility of collision during the reduction. Then, the distal fragment is rotated and translated to eliminate rotational and translational errors. Finally, the distal fragment is shortened until the reduction is complete.

## 2.2. Robot-musculoskeletal dynamic biomechanical model

We take the femur as an example because it is the most complex diaphysis and involves many muscles. The muscle used to provide power is distributed on the both sides of the motion axis of the joint in the form of mutual confrontation. A tough tendon connects the muscle to the bone. The ligaments attached to the bones limit the movement of the joint and maintain the stability of the bone, thereby enabling it to resist tensile forces without shrinkage. In conclusion, the main resistance to reduction comes from the muscle force. The muscles of the femur can be divided into three categories, the anterolateral group, the anteromedial group and the posterior group, for a total of 17 muscles. We simulate the muscle force using a muscle model. The muscle is described using the straight path method by a straight line that passes through the load-point. The position of the load-point is the center of the bone's surface area to which the muscles attach. The classical three element model of skeletal muscle proposed by A.V. Hill [18, 19] is adopted, as shown in Figure 2.

In the Hill model, the muscle is simplified to an active contractile element  $f_{ce}$ , a passive parallel

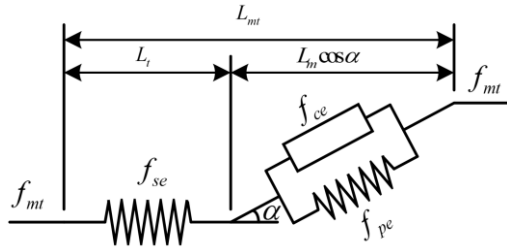


Fig. 2. Hill model of muscle force.

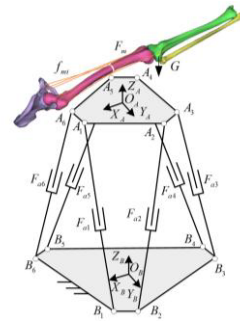


Fig. 3. Structural scheme of the reduction mechanism.

elastic  $f_{pe}$  and a series elastic element  $f_{se}$  to describe the tendons and muscles in series. The angle between them is described as the pinnation angle (PA)  $\alpha(t)$ . The muscle force  $f_{mt}$  and  $f_{se}$  are an instantaneous mechanical equality, with a relationship that can be described as

$$\begin{cases} f_{mt} = (f_{ce} + f_{pe}) \cos[\alpha(t)] \\ f_{mt} = f_{se} \\ \alpha(t) = \sin^{-1}\left(\frac{L_0 \sin \alpha_0}{L_m}\right) \end{cases} \quad (1)$$

In Eq. (1),  $\alpha_0$  is the PA when the muscle fiber is the optimal muscle fiber length, described by  $L_0$ .  $L_m$  is the muscle fiber length after stretching.

Before the robot-assisted fracture reduction, the patient is given strong relaxants that block the transmission of nerve impulses to the muscles. Only the stretched passive force of the muscle active force is effective, rather than the active force [20]. Therefore, based on the model modified by Zajac [21], each muscle force can be described by

$$f_{mi} = 1.3 f_{0i} \arctan \left[ 0.1 \left( \frac{L_{mi}}{L_{0i}} - 0.22 \right)^{10} \right] \cos \left[ \arcsin \left( \frac{L_{0i} \sin \alpha_{0i}}{L_{mi}} \right) \right] \quad (2)$$

In Eq. (2),  $L_{0i}$ ,  $f_{0i}$  and  $\alpha_{0i}$  are constants,  $i = 1, 2, \dots, n$ , where  $n$  is the number of muscles.

To analyze the dynamics of the robot-musculoskeletal skeletal, we fix the distal fragment and the moving platform of the Stewart mechanism together and take them as a whole, as shown in Figure 3. Some secondary factors, such as the muscle damping and the gravity of the driving rods, are ignored. The fragments are considered a rigid body. The deformation of the soft tissue does not significantly influence the mechanical properties of the bone movement. Kane method is fit for analyzing the rigid body such as the lower limb [22]. We just need to write a brief equation which is easy to solve. The complex calculation of internal force is also avoided. Based on this method, the dynamic equation of the robot-musculoskeletal system can be described by

$$M(\Theta)\ddot{\Theta} + C(\Theta, \dot{\Theta})\dot{\Theta} = J_{l,\bar{\Theta}}^T(\Theta) \cdot F_a + G(\Theta) + F_m \tag{3}$$

The left and the right sides of Eq. (3) are the generalized inertia forces and the generalized active forces, respectively.  $\Theta$  is the generalized pose vector. Let  $q_1, q_2, q_3, q_4, q_5$  and  $q_6$  be the values of translation and rotation in an inertial coordinate system  $O_B - X_B Y_B Z_B$ .  $\Theta$  can be described by

$$\Theta = [q_1 \quad q_2 \quad \dots \quad q_6]^T = [c^R \quad \beta^T]^T \tag{4}$$

$M$  is the mass matrix. We define  $m_p$  as the total mass of the distal fragment and the moving platform,  ${}^L I_p$  as the inertia matrix in  $O_B - X_B Y_B Z_B$  and  ${}^L R^U$  as the rotation transformation of  $O_A - X_A Y_A Z_A$  relative to  $O_B - X_B Y_B Z_B$ . The relationship between them can be described by

$$M(\cdot) = \begin{bmatrix} m_p \cdot E & 0 \\ 0 & {}^L I_p \end{bmatrix} \tag{5}$$

In Eq. (5):

$${}^L I_p = {}^L R^U \cdot {}^U I_p \cdot ({}^L R^U)^T \tag{6}$$

$C$  is the matrix of centripetal force and bathymetry. We define the coordinate matrix  ${}^L \tilde{\omega}$  as the corresponding matrix of the angular velocity  $\omega$  in  $O_B - X_B Y_B Z_B$ .  $C$  can be described by

$$C(\cdot) = \begin{bmatrix} 0 & 0 \\ 0 & {}^L \tilde{\omega} \cdot {}^L I_p \end{bmatrix} \tag{7}$$

$G$  is the matrix of gravity. We define  $g$  as the gravitational acceleration.  $G$  can be described by

$$G(\cdot) = [0 \quad 0 \quad m_p \cdot g \quad 0 \quad 0 \quad 0]^T \tag{8}$$

$J_{l,\bar{\Theta}}$  is the Jacobian matrix, which describes the relationship between the generalized velocity of the moving platform and the velocity of the output rods. We define  ${}^L l_n$  as the matrix of the output rods' unit length.  $J_{l,\bar{\Theta}}$  can be described by

$$J_{l,\bar{\Theta}}(\cdot) = [({}^L l_n)^T \quad ({}^L R^U \cdot {}^U A \times {}^L l_n)^T] \tag{9}$$

$F_a$  is the force of the output rods.  $F_m = [F_m'^T \quad M_m'^T]^T$  is the generalized force that acts on the

moving platform from the muscle force  $f_{mi}$ . The equation is established based on screw theory [23] to calculate  $F_m$ :

$$\sum_{i=1}^n f_{mi} \$_i = F'_m + \epsilon M'_m \quad (10)$$

In Eq. (10),  $F'_m$  is the principal vector of the force,  $M'_m$  is the principal moment, and  $\$_i$  is the unit line vector of the  $i$  th force:

$$\$_i = S_i + S_{0i} \quad (11)$$

Let  $d_i$  be the coordinates of the muscles in the distal fragment and  $p_i$  be the coordinates of the muscles in the proximal fragment. From Eq. (11),

$$\begin{cases} S_i = \frac{d_i - p_i}{|d_i - p_i|} \\ S_{0i} = \frac{p_i \times d_i}{|d_i - p_i|} \end{cases} \quad (12)$$

$F_m$  can be calculated as follows:

$$F_m = [G_{f_m}^{F_m}] f_m \quad (13)$$

In Eq. (13),

$$\begin{cases} f_m = [f_{m1}, f_{m2}, \dots, f_{mn}] \\ [G_{f_m}^{F_m}] = \begin{bmatrix} \frac{d_1 - p_1}{|d_1 - p_1|} & \frac{d_2 - p_2}{|d_2 - p_2|} & \dots & \frac{d_n - p_n}{|d_n - p_n|} \\ \frac{p_1 \times d_1}{|d_1 - p_1|} & \frac{p_2 \times d_2}{|d_2 - p_2|} & \dots & \frac{p_n \times d_n}{|d_n - p_n|} \end{bmatrix} \end{cases} \quad (14)$$

### 2.3. Simulation

We analyzed the dynamic biomechanical model by simulation using Matlab/Simulink (Matlab 2013a, MathWorks Co., Ltd, America). In the model, the lower-middle position of the femur is fractured, with the femur divided into two parts. The simulation is according to Eq. (3). The values of the muscle forces are based on Eq. (2). Some essential parameters are from references [10, 24], such as the optimal muscle fiber length, the maximum isometric contraction strength of the muscle and the PA when the muscle fiber is at the optimal muscle fiber length. Due to the fractured position, 8 muscles are involved in the model. The load-points of the muscles are presented in reference [25].

Table 1  
Pose of the distal fragment relative to the proximal fragment during the reduction

Action sequence	Direction that relative to the distal fragment	Direction relative to the coordinates of the robot	Value	Velocity
1	Stretched along the axial direction	Translated along the negative direction of the $X$ axis	20 mm	5 mm/s
2	Translated normal to the axial direction	Translated along the positive direction of the $Y$ axis	40 mm	5 mm/s
3	Rotated normal to the axial direction	Rotated along the positive direction of the $Z$ axis	30 degrees	8 degrees/s
4	Rotated along the axial direction	Rotated along the positive direction of the $X$ axis	30 degrees	8 degrees/s

The input of the model is the pose of the distal fragment relative to the proximal fragment. The muscle force and the forces of the output rods can thus be measured.

### 3. Results

According to the clinical path planning method of the fracture reduction, we take some typical values as inputs (Table 1) and run the procedure of the above model. The relationships between the poses of the distal fragment and the forces of the output rods are shown in Figures 4 and 5. The relationships between the poses of the distal fragment and the muscle forces are shown in Figures 6 and 7.

As shown in Figures 4 and 5, when the distal fragment is stretched, the variations of the output rods' forces are the most obvious. When the stretched length is 10 mm, the maximum force reaches about 200 N. When the stretched length is 20 mm, the maximum force reaches about 600 N. The variations of the forces are the slowest when the distal fragment translates normal to or rotates along its axial direction. The variations of the forces are between the above two when the distal fragment rotates normal to its axial direction. As shown in Figures 6 and 7, the variations of the muscle forces are the most obvious when the distal fragment is stretched, which are similar with the forces of the output rods. When the stretched length is 10 mm, the maximum force, which is the biceps femoris short head, reaches about 80 N. When the stretched length is 20 mm, this force is still the largest, reaches about

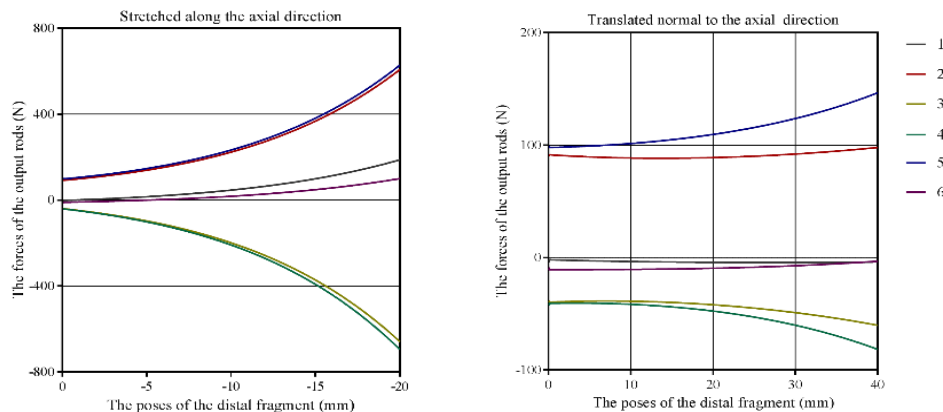


Fig. 4. Relationships between the poses of the distal fragment and the forces of the output rods (Translation).

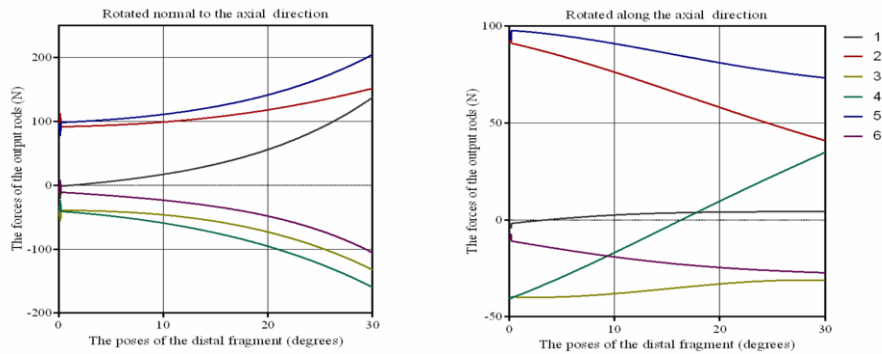


Fig. 5. Relationships between the poses of the distal fragment and the forces of the output rods (Rotation).

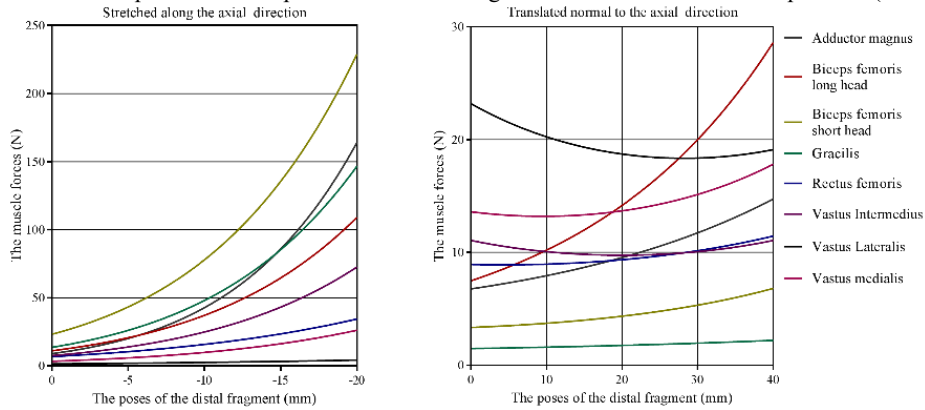


Fig. 6. Relationships between the poses of the distal fragment and the muscle forces (Translation).

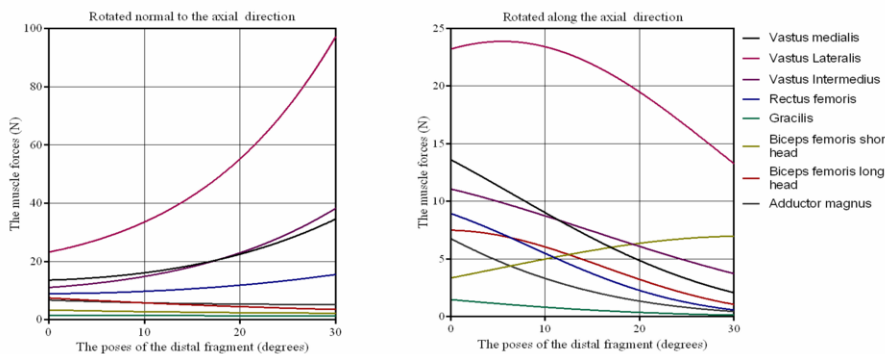


Fig. 7. Relationships between the poses of the distal fragment and the muscle forces (Rotation).

230 N. The variations of the forces are also the most slowest when the distal fragment translates normal to or rotates along its axial direction. The variations of the forces are between the above two when the distal fragment rotates normal to its axial. During the process of these above two motions, the force of the biceps femoris long head is the largest.

#### 4. Discussion and conclusions

Considering the safety factors for patients, this paper studied the robot-musculoskeletal biomechanical model, including the relationship between the muscle force, the force of the robot and the motion of the fragments. The influence of the muscle on the function of the robot in the reduction procedure is predicted and managed. It provides a useful reference for the mechanical design of the robot and the path planning of the fracture reduction.

Considering the characteristics of the Stewart mechanism and the muscle factors, we established a dynamic biomechanical model by using the Kane method. The Kane method is an effective method of solving complex dynamic problems using a computer, particularly for mechanical systems with multiple degrees of freedom. The results are obtained by simulation. From Figures 4-7, we can observe that the output forces are mainly caused by the muscle forces. Because the operation of the fracture reduction is a slow process, the acceleration and the velocity of the robot and the fragments are extremely low. The inertial force and the bathymetry have a small influence on the system. When the distal fragment is stretched, the variation of the muscle forces and the force of the output rods are the most obvious. We should therefore try to avoid the stretching operation. However, to avoid a collision between the fragments during the reduction, a certain stretching distance is necessary. Thus, 10 mm is the balance between the force and the interference, which is an acceptable value. When the distal fragment translates normal to its axis, it rotates normal to or along its axis. The variation of the muscle forces and the forces of the output rods are slow, making them relatively safe for patients. Some forces have a large influence on the system such as those of the biceps femoris short head and the biceps femoris long head. During reduction, proper poses should be ensured to reduce the effects of these muscles.

We adopted the Hill model to describe human muscle. As a classic model, its validity has been proven. We chose the straight path method to express the muscle motion, which reduces the complexity of the model by simplifying the calculation. For the general musculoskeletal model, inaccuracy could be introduced when the joints rotate. However, for the musculoskeletal model of fragments, there is no such problem because the relative displacements are not significant in reduction.

In actual fracture reduction, the parameters of patients are not completely the same as the standard data from the references that this study used. The forces of the output rods have some differences because the positions of the patients are fixed on the robot, but this does not significantly affect the trend of the muscle forces. This paper proposed a general solution method to guide fracture reduction.

Based on the results of this paper, we will study the robot path planning of fracture reduction. Due to the length of this paper and time limitations, together with the variability and the diversity of the robot-musculoskeletal system, we simplified some conditions and established a model to study instead of performing experiments. In this model, we simplified some conditions. In the next step, we will verify the dynamic biomechanical model by clinical experiments.

#### Acknowledgments

This research was supported by Natural Science Foundation of China (No. 61333019), Open Fund of State Key laboratory of Robotics and System (No. SKLRS-2013-MS-09) and National High-tech R & D Program (863 Program) (Nos. 2015AA0400614 and 2012AA041604).

## References

- [1] B. McKibbin, The biology of fracture healing in long bones, *The Journal of Bone and Joint Surgery* **60** (1978), 151-162.
- [2] I. Kempf, A. Grosse and G. Beck, Closed locked intramedullary nailing: Its application to comminuted fractures of the femur, *The Journal of Bone and Joint Surgery* **67** (1985), 709-720.
- [3] D.T. Gosling, R. Westphal, T. Hufner, J. Faulstich, M.J. Kfuri, F. Wahl, et al., Robot-assisted fracture reduction: A preliminary study in the femur shaft, *Medical and Biological Engineering and Computing* **43** (2005), 115-120.
- [4] R. Westphal, T. Gössling, M. Oszwald, J. Bredow, D. Klepzig, S. Winkelbach, et al., Robot assisted fracture reduction, *Springer Tracts in Advanced Robotics* **39** (2008), 153-163.
- [5] A.E. Graham, S.Q. Xie, K.C. Aw, W.L. Xu and S. Mukherjee, Design of a parallel long bone fracture reduction robot with planning treatment tool, 2006 IEEE/RSJ International Conference on Intelligent Robots and Systems, Beijing, China, 2006, pp. 1255-1260.
- [6] A.E. Graham, S.Q. Xie, K.C. Aw, W.L. Xu and S. Mukherjee, Robotic Long Bone Fracture Reduction, in: *Medical Robotics*, V. Bozovic, ed., INTECH Publisher, Vienna, Austria, 2008, pp. 85-102.
- [7] B. Füchtmeier, S. Egersdoerfer, R. Mai, R. Hente, D. Dragoi, G. Monkman, et al., Reduction of femoral shaft fractures in vitro by a new developed reduction robot system 'RepoRobo', *Injury* **35** (2004), 113-119.
- [8] T. Gössling, R. Westphal, J. Faulstich, K. Sommer, F. Wahl, C. Krettek, et al., Forces and torques during fracture reduction: Intraoperative measurements in the femur, *Journal of Orthopaedic Research* **24** (2006), 333-338.
- [9] L. Ren, Z. Qian and L. Ren, Biomechanics of musculoskeletal system and its biomimetic implications: A review, *Journal of Bionic Engineering* **11** (2014), 159-175.
- [10] S.L. Delp, J.P. Loan, M.G. Hoy, F.E. Zajac, E.L. Topp and J.M. Rosen, An interactive graphics-based model of the lower extremity to study orthopaedic surgical procedures, *IEEE Transaction on Biomedical Engineering* **37(8)** (1990), 757-767.
- [11] E.M. Arnold, S.R. Ward, R.L. Lieber and S.L. Delp, A model of the lower limb for analysis of human movement, *Annals of Biomedical Engineering* **38** (2010), 269-279.
- [12] S. Dosen, P. Popovski, J. Dideriksen, G. Pedersen and D. Farina, A novel technology for motion capture using passive UHF RFID tags, *IEEE Transaction on Biomedical Engineering* **60** (2013), 1453-1457.
- [13] A. Kinney, T. Besier, D. D'Lima and B. Fregly, Update on grand challenge competition to predict in vivo knee loads, *Journal of Biomechanical Engineering* **135** (2013), 021012.
- [14] B. Fregly, T. esier, D. Lloyd, S. Delp, et al., Grand challenge competition to predict in vivo knee loads, *Journal of Orthopaedic Research* **30** (2012), 503-513.
- [15] A.E. Graham, S.Q. Xie, K.C. Aw and W.L. Xu, Effects of dynamic forces in robotic fracture reduction, 2008 M2VIP 2008 15th International Conference on Mechatronics and Machine Vision in Practice, Auckland, New-Zealand, 2008, pp. 610-615.
- [16] H. Du, L. Hu, C. Li, T. Wang, L. Zhao, Y. Li, et al., Advancing computer assisted orthopaedic surgery using a hexapod device for closed diaphyseal fracture reduction, *The International Journal of Medical Robotics and Computer Assisted Surgery* (2014), doi:10.1002/rcs.1614.
- [17] C. Li, T. Wang, L. Hu, L. Zhang, H. Du, L. Wang, et al., Accuracy analysis of a robot system for closed diaphyseal fracture reduction, *International Journal of Advanced Robotic Systems* **11** (2014), doi: 10.5772/59184.
- [18] U. Glitsch and W. Baumann, The three-dimensional determination of internal loads in the lower extremity, *Journal of Biomechanics* **30** (1997), 1123-1131.
- [19] A. Soest and M.F. Bobbert, The contribution of muscle properties in the control of explosive movements, *Biological Cybernetics* **69** (1993), 195-204.
- [20] Z. Fe, Muscle and tendon: Properties, models, scaling, and application to biomechanics and motor control, *Critical Reviews in Biomedical Engineering* **17** (1989), 359-411.
- [21] S. Joung, S.S. Shikh, E. Kobayashi, I. Ohnishi and I. Sakuma, Musculoskeletal model of hip fracture for safety assurance of reduction path in robot-assisted fracture reduction, *International Federation for Medical and Biological Engineering (IFMBE) Proceedings* **35** (2011), 116-120.
- [22] T.R. Kane, Dynamics of nonholonomic systems, *Journal of Applied Mechanics* **28(4)** (1961), 574-578.
- [23] Z. Huang, Y. Zhao and T. Zhao, *Advanced Spatial Mechanism*, Higher Education Press, Beijing, 2006.
- [24] X. Zheng, *Modern Sports Biomechanics*, National Defence Industry Press, Beijing, 2007.
- [25] W. Sc, Y. Hj and W. Da, A three-dimensional musculoskeletal model for gait analysis, anatomical variability estimates, *Journal of Biomechanics* **22** (1989), 885-893.